THE JOURNAL OF COGNITIVE SYSTEMS
Journal Homepage:https://dergipark.org.tr/en/pub/jcs
Vol.7, No.1, 2022

Analysis of Heart Sound Signals in Ebstein's Anomaly

Omer Akgun

Marmara University Department of Computer Engineering, Faculty of Technology, Istanbul, Turkey. (e-mail:oakgun@marmara.edu.tr).

ARTICLE INFO

Received: March, 03.2022
Revised: April, 09.2022
Accepted: May, 19.2022

Keywords:
Ebstein's anomaly , Heart sound signals, Time frequency analyses, Bispectrum, Power spectrum density.

Corresponding author:Ömer Akgün
✉ oakgun@marmara.edu.tr
☎+90 216 777 38 04

ISSN:2548-0650

DOI: https://doi.org/10.52876/jcs.1131979

ABSTRACT

Ebstein's anomaly is an abnormality in the pediatric heart disease group. The anomaly is described as a structural defect by considering the whole heart. It can be manifested by typical symptoms in auscultation and can be detected with other diagnostic methods such as ECG. Systolic ejection click and murmur are the most important symptoms in the diagnosis of disease. In this study, heart sound signal recorded from a 13-year-old patient was analyzed with different numerical methods along with a normal heart sound signal. The signals were first examined in the time plane and findings in auscultation were observed. The frequency components of the signals were then obtained. Additional frequency components emerged in findings of disease in this plane compared to the normal one. Spectrograms enable to observe the differences in time frequency and amplitude components. Bispectral analysis was performed as a high order spectral analysis method by diversifying the analysis. In bispectral analysis of the anomaly, click and murmurs are manifested by equiphase surfaces distributed at high frequencies.Lastly, the power spectrum density of the signals were examined. The decrease in the additional power peak and power rating of the diseased signal was remarkable.

1. INTRODUCTION

EBSTEIN'S anomaly is a quite rare anomaly which is seen in <1% of all congenital heart diseases. It was first described by Wilhelm Ebstein in 1866.

Ebstein's anomaly is an anomaly in the tricuspid valve. The tricuspid valve separates the right atrium (the chamber where blood returns to the heart from the body) from the left ventricle (the chamber which pumps blood to the lungs).

In Ebstein's anomaly, two leaflets of the tricuspid valve were displaced towards the apex (end) of the right ventricle. Due to this displacement, the right ventricular cavity was narrowed and the right atrium was enlarged. The displacement of these cavities is called atrialization of the right ventricle. The third leaflet is elongated and may be tethered to the wall of the cardiac cavity. Rarely, the valve is so deformed that it will not allow blood to flow easily forward in the normal direction.

More commonly, these anomalies cause the blood to escape backwards from the tricuspid valve to the right atrium when the right ventricle contracts. As a result, the right atrium becomes enlarged (Figure 1). If the tricuspid regurgitation (leakage) is sufficiently serious, it may result in congestive heart failure and enlarged heart.

Normally, there is a connection or hole between the right and left atrium in the fetus, which is also known as foramen ovale or PFO. The PFO usually closes after birth.

In Ebstein's anomaly, the high pressure in the right atrium keeps the PFO open. This connection provides the blood with low oxygen content to pass from the right atrium to the left atrium, bypass the lungs and disperse directly into the body. This results in low level of oxygen in the blood. That is why children with Ebstein's anomaly become blue (cyanotic) and have low level of oxygen saturation [1-5].

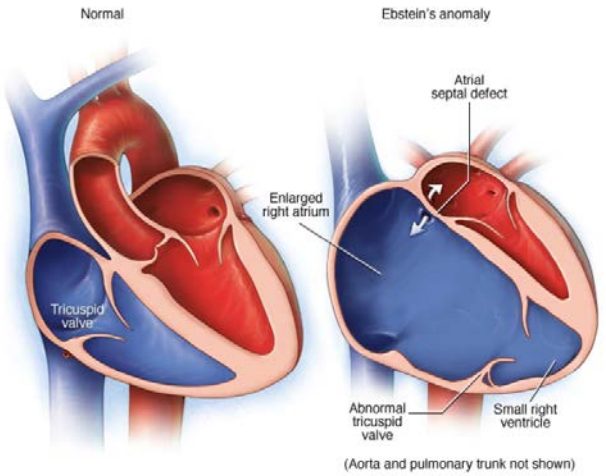

Fig. 1. Normal Heart (left) Heart with Ebstein's anomaly (right) [6].

The most obvious finding in auscultation is the mating of S_1 due to a delay in the closure of the large anterior tricuspid leaflet. The delay in tricuspid valve closure depends on mechanical causes rather than the right bundle branch block. An opening sound may be also heard in the diastole depending on the large anterior leaflet. Atrial S_4 and S_3, if there is a heart failure, may be also heard. The pulmonary component of S_2 may be delayed and soft due to the right bundle branch block or may not be heard due to the low level of PAP (pulmonary artery pressure). Pansystolic murmur

may be heard in the left sternal margin in 1/3 of the patients depending on the tricuspid valve insufficiency. Also, diastolic murmur may be heard due to the blood flow through the malformed tricuspid orifice [7].

Heart sounds are first recorded with a digital stethoscope from proper points through the chest and in a quiet environment (Figure 2). The tricuspid focus is located on the margin of the left side sternum (breastbone), the fourth intercostal space on the left side of the sternum. Tricuspid and right heart sounds are the best heard in this region [8].
Then, the recorded sound signals are transferred to the computer via an infrared receiver and the digital data is converted to be analyzed (such as audio file format conversion, noise filtering).

Fig. 2. Recording heart sounds with a digital stethoscope [8].

When the signals of the filters, electronic systems such as amplifiers or biological systems such as EEG, EMG, ECG and PCG are examined, it is very important to know the Amplitude-Frequency and Phase-Frequency characteristics of these systems in order to familiar with it.
As PCG signals are very complex, their strict properties can be only determined with appropriate signal processing techniques. When these signals were accepted as stationary signal and spectrum analyses were performed; they were accepted as non-stationary signals and time-frequency analyses were performed.

The simplest method in signal analysis is time-amplitude. However, it is a useful method to easily observe the harmonization of heart sounds with auscultation.

In the 19th century, the French mathematician J. Fourier showed that any periodic function could be expressed with the sum of unlimited number of complex exponential periodic functions. After the intervening years, it was found that the non-periodic functions could be also expressed in this way by generalizing Fourier's ideas [9].
The Fourier transform of the numerical signals obtained in the study also gives the frequency spectrum of the signal and it is determined which frequency components are intense in the signal.

In 1946, the Gabor Transform, which was proposed by Gabor, MD, working in the field of communication, allowed the regional frequency analysis to be performed by taking the Fourier Transform of any signal scanned with time translation of a constant function defined as the window function. In this case, the Fourier Transform of the windowed signal also includes time information as well as the frequency components of the signal. The window function used in the transformation is the Gaussian function, which is limited in time and frequency domains. With a new algorithm introduced in 1965, the Gabor Transform was also extended to the "Short-Time Fourier Transform" (STFT), which uses different window functions. This form of transformation is a very useful solution especially for computer applications [10].

In signal processing methods using the second-order statistics and/or power spectrum, the phase relations between the frequency components are not considered; therefore, these methods are blind to phase information.
The higher order statistics are used to examine gauss, stationary and non-linear processes and obtain significant results.

The high order spectral analysis (HOSA) can provide more information from these processes. The most effective use of HOSA is to reveal the characteristics of noise signals that do not show the Gaussian distribution as it resets the Gaussian distributed noise processes [11].
In this study, ebstein's anomaly was analyzed by using bispectral analysis as a HOSA method.

2. TIME-FREQUENCY-AMPLITUDE ANALYSES

The signal $x(nT)$ obtained by sampling a continuous-time $x(t)$ signal at $t=nT$ is called a discrete-time signal. Where T is the sampling period and n is also an integer. Therefore, the discrete-time signals consist of a series of numbers.
Any discrete-time signal can be written in form of the sum of the series of the multiplied and iterated unit impulses (equation 1) [6-10].

$$x(n)=\sum_{k=-\infty}^{\infty} x(k)\delta(n-k) \qquad (1)$$

Similarly, a continuous x(t) heart sound signal also can be saved to a recorder and transferred to a computer environment by making it discrete with a certain sampling frequency [8].

Such a $x(t)$ heart sound signal that was recorded from a healthy heart and one cycle took approximately 0.8 seconds was sampled with a sampling frequency of 11025 Hz and one cycle was drawn with n = 8900 samples. This duration consisted of a systole (0.3 seconds) and diastole (0.5 seconds); this graph was shown in Figure 3. S_1 (at the beginning of the systole) and S_2 (at the beginning of the diastole) represent two basic components of the normal heart sound signal.

The graph in Figure 4 was taken from a 13-year-old patient with Ebstein's anomaly with severe tricuspid insufficiency. The record was made from the left lower margin of the sternum. When the graph is examined, there is a systolic murmur (SM) due to a systolic ejection click (EC) and tricuspid insufficiency. The pulmonary component (PC) of S_2 is delayed and its severity is depressed; there is also a diastolic murmur (DM) due to tricuspid stenosis caused by an increase in the volume of blood flow from the tricuspid valve in the diastole. The second more important quantity is also "frequency" along with time. The signals are mathematically defined by Fourier in the form of frequency. According to this definition, the signals can be represented as a linear combination of a fundamental frequency and the harmonic frequencies of that fundamental frequency with different amplitudes.

 ISSN: 2548-0650 http://dergipark.gov.tr/jcs

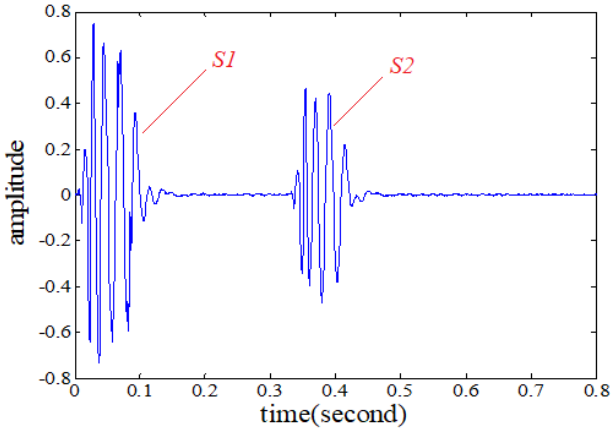

Fig. 3. Time-amplitude graph of a cycle of a healthy heart sound signal.

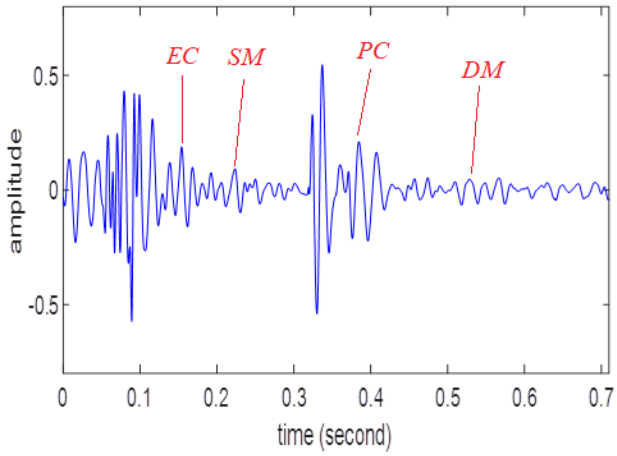

Fig.4. Time-amplitude graph of heart sound signal in Ebstein's Anomaly

Time-frequency analysis is considered the most basic and necessary analysis. As there are many different methods for generating time-frequency distributions, it is necessary to classify them as Linear time-frequency distributions and Quadratic time-frequency distributions based on their structures and characteristics. The Short-Time Fourier Transform (STFT) and Wavelet Transform (WT) are examples of Linear time-frequency distributions. Examples of quadratic time-frequency distributions are spectrogram, scalogram (WT amplitude squared), Wigner Distribution (WD) and generally Cohen's class time-frequency distributions. The Fourier transform of a discrete-time signal gives its frequency spectrum and it is determined which frequency components are intense in the signal.

The Discrete-Time Fourier Transform (DTFT) of the discrete-time signals is given in Equation (2).

$$X(\Omega) = \sum_{n=-\infty}^{\infty} x(n) e^{-j\Omega n} \tag{2}$$

The Amplitude and phase sections and fourier spectrum of the signal can be defined in Equation (3). The Discrete Fourier Transform of a signal is also shown in Equation (4).

$$X(\Omega) = |X(\Omega)| e^{j\angle X(\Omega)} \tag{3}$$

$$X[k] = \sum_{n=0}^{N-1} x(n) e^{-j(2\pi/N)kn} \qquad k = 0,1,\ldots\ldots,N-1 \tag{4}$$

As the Discrete Fourier Transform (DFT) is defined as the calculation of the N number(s) of frequency value(s) from the Discrete-Time Fourier Transform (DTFT), it corresponds to the sampling of DTFT in the frequency domain. It is possible to calculate the DFT faster by the symmetry and periodicity properties of the phase factor (Equation 5) in the Discrete Fourier Transform.

$$W_N = e^{-j(2\pi/N)} \tag{5}$$

The decimation in time and decimation in frequency methods are called the Fast Fourier Transform (FFT) and in practice, FFT is always used [12-14].

In Figure 5, the frequency distribution of 15 to 150 Hz is observed in the healthy heart sound signal. It appears to be a peak up to max. 3000 units of amplitude at 45 Hz and then down to 150 Hz.

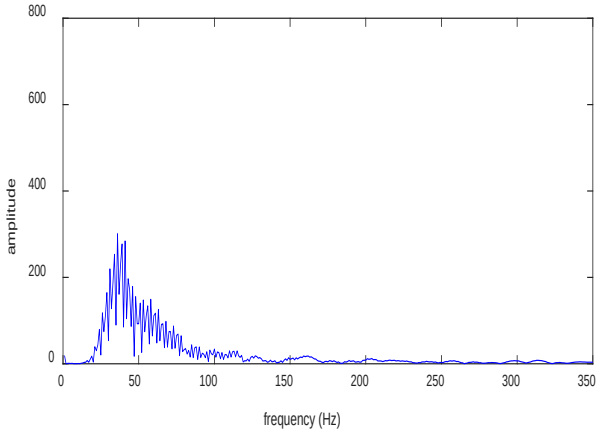

Fig. 5. Healthy heart sound signal amplitude spectrum.

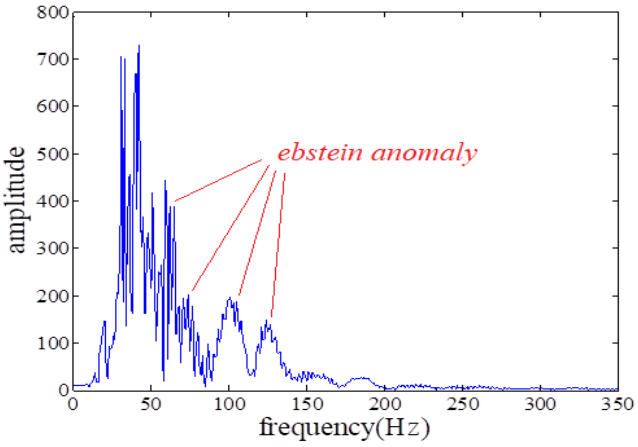

Fig.6. Frequency-amplitude graph of heart sound signal in Ebstein's Anomaly.

In Figure 6, there is the cluster of components peaking at (30,705), (40,730) points and (60,450) (75, 90) points at approximately the range of 20-80 Hz, and then components with smaller amplitude at the range of 90-110 Hz and 120-140 Hz [respectively peaking at (100,192) and (125,148) points].

The Short-Time Fourier Transform (STFT) is obtained by taking the classical fourier transform of the signal divided by a sliding window in time. Spectrum estimation can be performed by assuming that the the portion of the examined signal taken with the window remains stationary.

Once the signal is passed through a window defined in the time domain, FT is applied. The window function is shifted along the time axis to include the whole signal so that the frequency responses (frequency spectra) of the signal are obtained at the time intervals in the width of the window function. In this way, it may be obtained the the frequency response of the signal changed over time. The formula that provides the STFT transformation is given in Equation (6).

$$STFT(\tau, f) = \int_{-\infty}^{\infty} [x(t).w^*(t-\tau)].e^{-j2\pi ft} dt \quad (6)$$

Where $x(t)$ is the basic signal, $w(t)$ is the window function * complex conjugate notation, time translation. The STFT consists of the FT of the signal multiplied by a window function. A new STFT coefficient set is calculated for each t and f. As it is, FT is only a function of frequency but STFT is a function of both frequency and time, and is thus three-dimensional (the third dimension is amplitude) [15, 16].

The normal signal is behind 0.1 sec, with an energy density reaching its highest value around 50 Hz and down to 150 Hz, and with maximum amplitude around 45 Hz and energy zones down to 200 Hz at the both sides of 0.4 sec (S1 and S2 energy zones). S_1 lasts for 0.1 sec and S_2 is up to 0.08 sec (Figure 7).

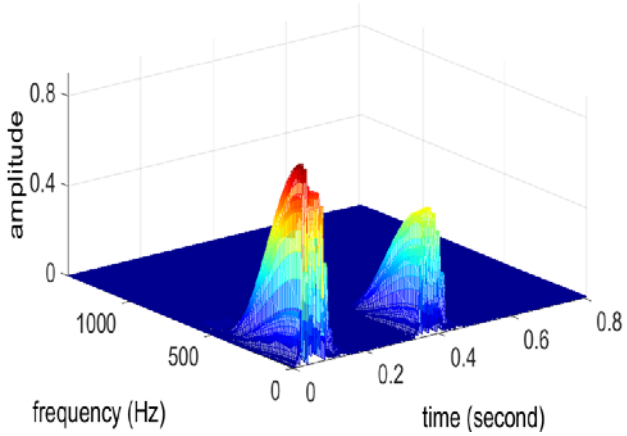

Fig.7. 3-Dimensional spectrogram of the normal heart sound signal.

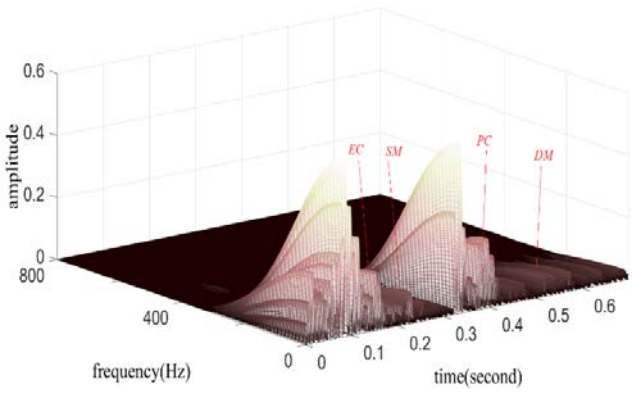

Fig. 8. Heart sound signal spectrogram in Ebstein's Anomaly

There is a systolic ejection click right next to the basic component of S1 in Figure 8. It is seen in a region around 60 Hz as a frequency. Also, systolic murmur is a pathological finding in this region. The pulmonary sound, which forms the basic component of S2 extends to 100 Hz for about 0.4 sec. This is followed by diastolic murmur peaks.

3. BISPECTRAL ANALYSIS

The bispectrum reveals the signals of the non-linear process, as well as the suppression of the Gaussian probability distribution activity. The bispectral analysis is used to detect low-level but diagnostically important signals which are masked by background FKG.

If the power spectrum of random signals is defined with DFT as like in Equation (7), the 3rd order population spectrum is also called bispectrum. The bispectrum is shown in Equation (8). If the signal is a reel value and stationary random, it is shown as like in Equation (9) [17-20].

$$P_2^x(f) = DFT(C_2^x(m).e^{-j2\pi mf} \quad (7)$$

$$B^x(f_1, f_2) = \sum_{m=-\infty}^{\infty} \sum_{n=-\infty}^{\infty} C_3^x(m,n).e^{-j2\pi(mf_1+nf_2)} \quad (8)$$

$$B(w_1, w_2) = X(w_1).X(w_2).X^*(w_1+w_2) \quad (9)$$

In Figure 9, there are the rings with low power density (the 1st order) at high frequencies for a normal heart, and the nested power density rings (the 1st, 2nd, 3rd and 4th order) ascending from low to high at lower frequencies.

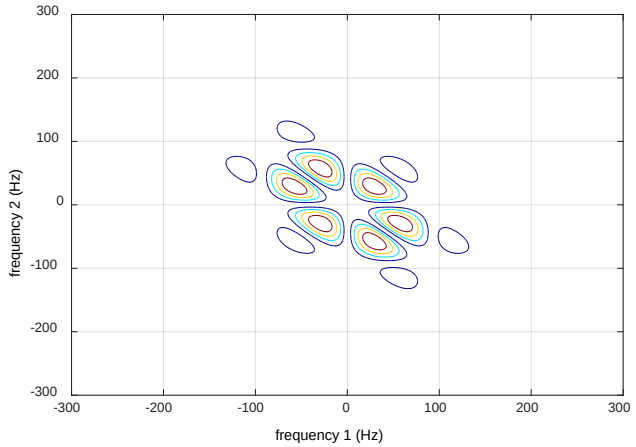

Fig. 9.Normal heart sound signal bispectrum

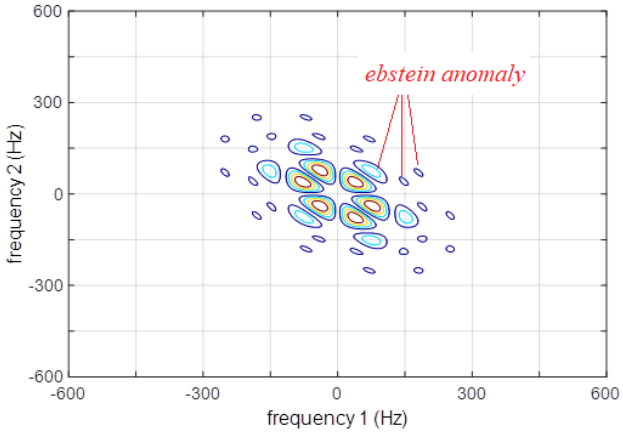

Fig. 10. Bispectral Analysis

In Figure 10, the bispectrum is surfaces with high amplitude, which occurs in the second power density rings that characterize the anomaly in the equiphase surface (light blue inner rings). Moreover, we also monitor the murmurs specific to anomaly in the ring group with low amplitude.

4. POWER SPECTRUM DENSITY (PSD)

The purpose of Spectral estimation in signal analysis is to determine the distribution of a signal strength based on frequency. The methods of PSD estimated directly from the signal itself are called non-parametric; the methods that the input is obtained from the output of a linear system driven by a white noise are called parametric. Subspace methods are also known as high resolution methods. This method provides to make the frequency component estimates based on the Eigen analysis for the correlation matrix of a signal. Subspace methods are also known as high resolution methods. This method provides to make the frequency component estimates based on the Eigen analysis for the correlation matrix of a signal [21]. Multiple signal classification (MUSIC) and Eigen-Vector (EV) methods are among the methods included in this category. These methods are particularly suitable for the generation of the spectra of sinusoidal signals and are particularly effective in identifying low signal-to-noise ratio, noise-embedded sinusoids [22].
MUSIC (multiple signal classification) method is a subspace frequency estimator proposed by Schmidt, and eliminates the effect of spurious zeros by using the averaged spectrum of all the eigenvectors corresponding to the noise subspace.
The power spectrum density (PSD) is obtained from the statement in equation 10.

$$P_{MUSIC}(f) = \frac{1}{1/K \sum_{i=0}^{K-1} |A_i(f)|^2} \tag{10}$$

Where K is the dimension of the noise subspace, A_i means all the eigenvectors of the noise subspace.
The eigenvector method allows the calculation of a desired noise subspace vector from noise or signal subspace eigenvectors by forcing spurious zeros into the unit circle in order to differentiate spurious zeros from real zeros.
The power spectral density is obtained from the statement in Equation 11 with the eigenvector method [23, 24].

$$P_{ev}(f) = \frac{1}{\left(\sum_{i=0}^{K-1} |A_i(f)|^2 / \lambda_i \right)} \tag{11}$$

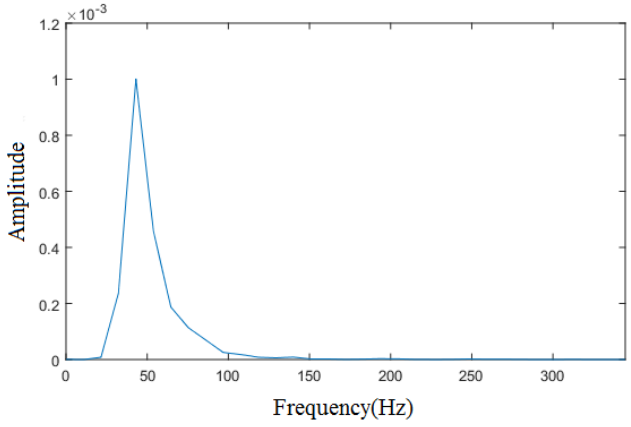

Fig. 11. The PSD of normal heart sound signal.

There was a curve peaking at approximately 0.001 units at 45 Hz and descending to zero at 125 Hz at the normal signal PSD in Figure 11.

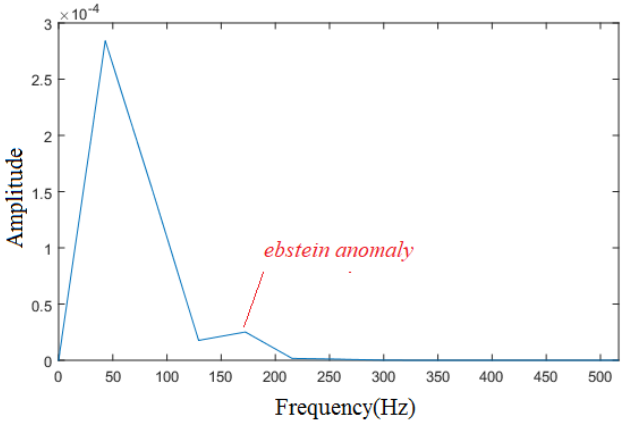

Fig. 12. Power Spectrum Density of Ebstein's Anomaly

There was a very high power decrease in the ebstein power spectrum compared to the normal in Figure 12 (0.00028 units). A small power zone was formed in the 125-225 Hz region (max. 0.000025).

5. CONCLUSIONS

The The pulmonary component and diastolic murmur were observed to be significantly reduced and delayed in terms of the systolic ejection click in the time-dependent change of Ebstein's anomaly and the amplitude in the holosystolic murmur diastole.
The anomaly varies between approximately 0-250 Hz in the time-frequency graph. The anomaly showed itself with the cluster of components peaking at the points of (60,490), (75,90), (100,192) and (125,148).

There was an ejection click extending to 60 Hz for about 0.18 sec at the spectrogram. There is also a holosystolic murmur extending to 100 Hz. The pulmonary component which was prominently separated from the aortic component and decreased its amplitude extends to 80 Hz for about 0.4 sec. Subsequently, diastolic murmurs were observed.
When the bispectrum was examined, the low-amplitude peaks were seen in the second rings. Moreover, additional two groups of low-peak rings were formed on the equiphase surfaces in ebstein's anomaly.

There was a huge decrease in power components in the PSD graph. The peaks with maximum amplitude of 2.8,10-4 were formed around 50 Hz. Also, the peak is remarkable at the 125-225 Hz region as another finding showing the anomaly.

REFERENCES

[1] A.F. Corno, P.G. Chassot, M. Payot, N. Sekarski, P. Tozzi, L.K.V. Segesser, “Ebstein’s anomaly. One and a half ventricular repair”, Swiss med wkly, Vol.132, pp. 485-488, 2002.
[2] J.B. Seward, “Ebstein's Anomaly: Ultrasound Imaging and hemodynamic evaluation”, Echocardiography. A Journal of CV Ultrasound. Allied-Tech 6, pp. 641, 1993.
[3] E.A. Jeyman, *Principles and Practice of Echocardiography*, Lea-Febiger, Pennsylvania, pp. 840, 1994.
[4] R.A. Lange, J.E. Cigarroa, Conn's Current Therapy , pp.105-110 , 2019.
[5] https://www.drtaneryavuz.com/ebstein-anomalisi/, 2021
[6] https://www.mhttpayoclinic.org/diseases-conditions/ebsteins-anomaly/symptoms-causes/syc-20352127, 2021.

[7] D.P. Singh, K. Mahajan, StatPearls [Internet],StatPearls Publishing, Treasure Island (FL), 2018.
[8] O. Akgun, Analysis of heart sound signals in mitral valve diseases, PhD thesis, 2011.
[9] G.E. Guraksin, E. Ucman, O. Deperlioglu, "Performing discrete fourier transform of the heart sounds on the pocket computer", 14th National Biomedical Engineering Meeting, 2009.
[10] E. Onal, J. Dikun, "Short-Time Fourier Transform for Different Impulse Measurements", Balkan Journal of Electrical and Computer Engineering (Bajece), Vol.1, No.1, pp.44-47, 2013.
[11] M. Mishra, S. Pratiher, S. Banerjee, A. Mukherjee, "Grading heart sounds through variational mode decomposition and higher order spectral features", 2018 IEEE International Instrumentation and Measurement Technology Conference (I2MTC).
[12] R. Bracewell, The Fourier transform and its applications. *3rd edn*. McGraw-Hill, New York, 1999.
[13] S.K. Mitra, J.F. Kaiser, Handbook for Digital Signal Processing, John Wiley & Sons, NY, NY, 1993.
[14] A.L.Douglas, "The Discrete Fourier Transform, Part 4: Spectral Leakage", in Journal of Object Technology, Vol.8, No.7, pp. 23-24, 2009.
[15] P.B. Marchant, "Time-Frequency Analysis for Biosystem Engineering", Biosystems Engineering, Vol.85, No.3, pp. 261-281, 2003.
[16] A. Parkhi, M. Pawar, "Analysis of Deformities in Lung Using Short Time Fourier Transform Spectrogram Analysis on Lung Sound", International Conference on Computational Intelligence and Communication Networks, 2011
[17] Y.C. Kim, E.J. Powers, "Digital Bispectral Analysis and it's Applications to Nonlinear Wave Interactions", IEEE Transactions on Plasma Science, Vol.7, No.2, pp. 120-131, 2007.
[18] T.C. Akinci, S. Seker, O. Akgun, J. Dikun, G. Erdemir, "Bispectrum and energy analysis of wind speed data", 2016 The 9th International Conference on Computer and Electrical Engineering (ICCEE 2016), Barcelona, December, 2016.
[19] C.L. Nikias and M.R. Raghuveer, "Bisepctrum Estimation: A Digital Signal Processing Framework", Proceedings of the IEEE, Vol.75, No.7, pp. 869-891, 1987.
[20] J.T. Astola, K.O. Egiazarian, G.I. Khlopov, S.I. Khomenko, I.V. Kurbatov, V.YE. Morozov, A.V. Totsky, "Application of bispectrum estimation gor time-frequency analysis of ground surveillance Doppler radar echo signals", IEEE Trans. on Instrumentation and Measurement, Vol.57, No.9, pp.1949–1957, 2008.
[21] M. Zainuddin Lubis, *Signal processing for marine acoustic and dolphin using matlab, Edition: 2016, Chapter: 2*, Publisher: LAP LAMBERT Academic Publishing is a trademark of OmniScriptum GmbH & Co. KG, Editors: Carolyn Evans, pp.15-25, 2016.
[22] E.D. Ubeyli, I. Guler, "Comparison of eigenvector methods with classical and model-based methods in analysis of internal carotid arterial Doppler signals", Computers in Biology and Medicine. Vol.33, pp. 473–493, 2003.
[23] P.S. Akanksha, M. Kayapanda, S. Goutam, "Identification of Coronary Artery Disease using Cross Power Spectral Density", 14th IEEE India Council International Conference (INDICON), 2017.
[24] N. Lahcène, A. Hafaifa, A. Kouzou, M. Guemana, S. Abudura, "Detecting rotor faults of SCIG based wind turbine using PSD estimation methods", 8th International Conference on Modelling, Identification and Control (ICMIC), 2016.

BIOGRAPHIES

Omer Akgun is an assistant professor at the, Department of Computer Engineering, Technology Faculty, Marmara University. He received his first Ph.D. in the Communication Engineering in 2009 from Yildiz Technical University and the second Ph.D. in the Electronic and Communication Education Department in 2011 from Marmara University. His current research interests are signal processing, biomedical signal processing, signal modelling and communication systems.